Zeitschrift: Schweizerische mineralogische und petrographische Mitteilungen = Bulletin suisse de minéralogie et pétrographie

Band: 85 (2005)

Heft: 1

Artikel: Permian zircon U-Pb ages in the Gran Paradiso massif : revisiting post-Variscan events in the Western Alps

Autor: Bertrand, Jean-Michel / Paquette, Jean-Louis / Guillot, François

DOI: https://doi.org/10.5169/seals-1651

Schweizerische Mineralogische und Petrographische Mitteilungen 85, 15–29, 2005

Permian zircon U–Pb ages in the Gran Paradiso massif: revisiting post-Variscan events in the Western Alps

Jean-Michel Bertrand[1*], *Jean-Louis Paquette*[2] and *François Guillot*[3]

Abstract

In the Internal Western Alps, the Gran Paradiso massif is an eclogitic gneiss dome of Alpine age. It is largely composed of porphyritic metagranites which have long been interpreted as Variscan intrusives in a pre-Variscan basement. Strong deformation and metamorphism affected the entire massif during the Alpine orogeny. The present study confirms earlier, preliminary results that suggested a mid-Permian age for some of the granitic protoliths, thus postdating the last Variscan orogenic granitoids. We also extend that result to the bulk of the massif, from the top contact near Bonneval (Arc valley, France) to the structurally deepest part in Noasca (Orco valley, Italy). Six new U–Pb age determinations were carried out on zircons (IDTIMS and SHRIMP) from four porphyritic orthogneisses and two samples of host rocks with magmatic affinities. All ages are Permian, ranging from 264 to 277 Ma. The oldest ages pertain to the Noasca granite, in the core of the dome, and to a massive gneiss (Bivacco Carpano) that belongs to the main pre-granite metasedimentary and metavolcanic pile. Similar ages were obtained for granites and their host rocks, suggesting that a large part of the Gran Paradiso dome consists of volcanics, volcano-clastic rocks and granites of Permian age, rather than earlier Variscan assemblages. From their dominantly Permian protoliths, Gran Paradiso and other Piemonte massifs (Monte Rosa and Dora Maira), which are part of the Internal Crystalline Massifs, are very different in paleogeographic significance from the External Crystalline Massifs, which represent the European basement, where Permian magmatism is sparse. The Piemonte basement massifs may represent the easternmost edge of a Briançonnais – Grand-Saint-Bernard allochthonous terrane with more affinity to the Apulian basement than to the European basement.

Keywords: Gran Paradiso, zircon dating, protolith ages, Permian, paleogeography, pre-Alpine basement.

1. Introduction

Alpine geologists traditionally have favoured the study of Mesozoic and Cenozoic rocks and events, pertaining to the Alpine cycle. However, maps and cross-sections of the Alpine belt show a predominance of Paleozoic rocks (Michard and Goffé, 2005). To fully decipher the structure and history of such a polyorogenic belt, some knowledge of the age of its basement protoliths is required. Increasingly precise techniques for U–Pb dating of zircon (Davis et al., 2003) have provided a wealth of reliable protolith ages during the last fifteen years. The present work is aimed at filling an important gap among the deepest units of the Alps, which have been studied more extensively for their Alpine high-pressure metamorphism than for the age of their protoliths.

In the Western Alps, the Internal Crystalline Massifs (ICM) comprise, from W to E (Fig. 1), the Briançonnais Grand-Saint-Bernard basement massifs (GSB), the Piemonte massifs, namely the eclogitic gneiss domes of Monte Rosa (MR), Gran Paradiso (GP) and Dora Maira (DM), which outcrop below the Liguria-Piemonte „Schistes Lustrés" oceanic units (SL), and the Sesia continental basement classically attributed to the Austro-Alpine units derived from the Apulian plate.

Gran Paradiso orthogneisses were previously considered to derive from Variscan granitoids (Bertrand, 1968, Callegari et al., 1969, Borghi et al., 1994, Vearncombe, 1983) but Permian ages have recently been reported for the westernmost part of the massif (Bertrand et al., 2000b). The main goal of the present study was to check if

[1] Laboratoire de Géodynamique des Chaînes Alpines – LGCA-CNRS, Campus universitaire, Université de Savoie, F-73376 Le Bourget-du-Lac cedex, France. *Corresponding author* <jimmy.bertrand@wanadoo.fr>
[*] Present address: 15 chemin d'Avat, F-38240 Meylan, France.
[2] Laboratoire de Géologie, UMR6524 „Magmas et Volcans", Université B. Pascal, 5 Rue Kessler, F-63038 Clermont-Ferrand cedex, France.
[3] UMR Processus et Bilans des Domaines Sédimentaires, Université des Sciences et Techniques de Lille 1, F-59655 Villeneuve d'Ascq Cedex, France.

0036-7699/05/0085/15

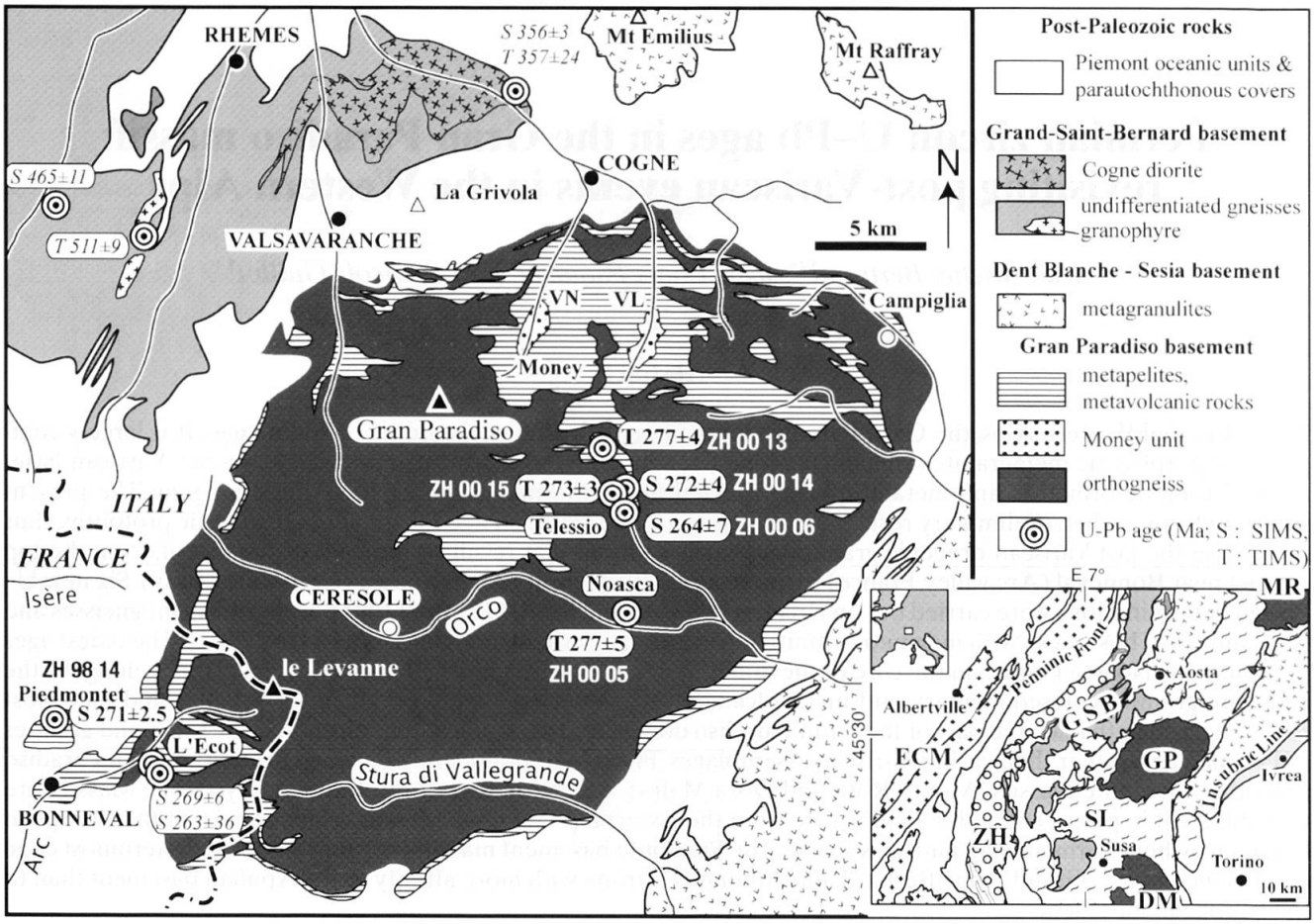

Fig. 1 Sketch map of the Gran Paradiso massif with sample locations. Map adapted from Bertrand (1968) and Compagnoni et al. (1974). Inset: External Crystalline Massifs (ECM), crosses; Upper Carboniferous and Permian series of „Zone Houillère" (ZH), circles; Grand-Saint-Bernard basement massifs (GSB), middle grey; oceanic units with „Schistes Lustrés" (SL), tildes; other Mesozoic to Recent formations, white; Piemonte basements (MR: Monte Rosa, GP: Gran Paradiso, DM: Dora Maira), dark grey; Ivrea Zone, pale grey. Previously published ages shown in italics (Bertrand et al., 2000a,b; Guillot et al., 2002).

other orthogneisses occurring in the massif may be older. After an overview of the geology of the Gran Paradiso massif, this paper presents new U–Pb data confirming the predominance of Permian protoliths. In the discussion a short review of the Permian paleogeography of the different tectonic units of the internal Western Alps is attempted.

2. Geological setting

2.1. Rock-types and main structure of the Gran Paradiso massif

Like Monte Rosa (MR) and Dora Maira (DM), the Gran Paradiso (GP) massif corresponds to the deepest structural level exposed in the Western Alps. GP rocks experienced high-pressure metamorphic conditions estimated in the range 450–550 °C / 9–16 kbar (Brouwer et al., 2002 and references therein). The GP massif is a dome defined by the Alpine foliation and made up dominantly (more than 60% in volume) of massive orthogneisses (Fig. 1). In addition, the massif contains metasediments with subordinate greenstones preserving eclogitic assemblages (Compagnoni and Lombardo, 1974; Dal Piaz and Lombardo, 1986; Brouwer et al., 2002). On top of the dome, discontinuous lenses of cover rocks comprise quartzites, grey dolomite and banded marbles, the protoliths of which have classically been considered Triassic to Cretaceous in age (Elter, 1972). In the Valnontey and Valeille valleys (VN and VL on Fig. 1), tectonic windows – the Money window in Valnontey – were recognized (Compagnoni et al., 1974; Ballèvre, 1988), based on the presence of a conspicuous conglomerate horizon and of graphite schists. At the western end of GP, the „série de Bonneval" is a monotonous albite-phengite gneiss unit, attributed to the Permian on the basis of its felsic volcanic origin (Bertrand, 1968).

The Alpine foliation is penetrative in all rock types. Figure 2 is a sketch of the massif, showing a thick upper slab of orthogneiss (forming the Gran

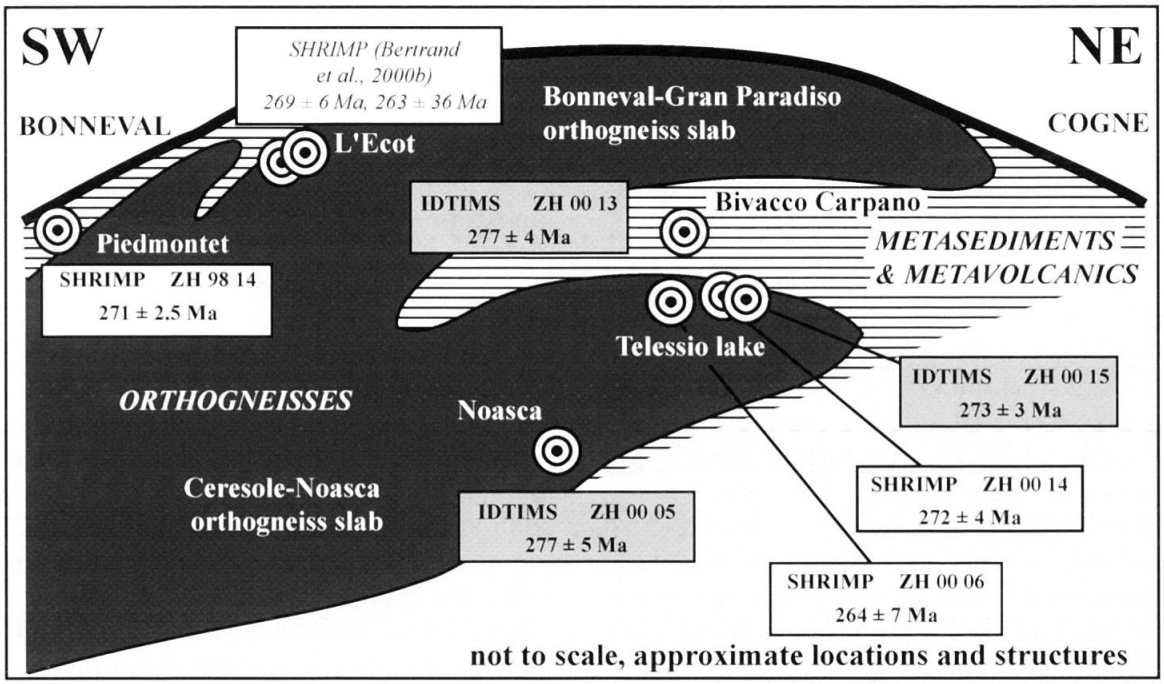

Fig. 2 Sample location on a sketch section of the Gran Paradiso. Section inspired from Compagnoni et al. (1974) and from mapping by one of the authors (JMB).

Paradiso summit), which tops a domain towards the North where metasediments dominate (Valnontey, Valeille and Campiglia on Fig. 1). A lower orthogneiss slab constitutes the lower slopes of the Orco valley, and the two slabs merge toward the south where they form the huge 2300 m high wall that terminates the Stura di Vallegrande valley. E–W-trending Alpine folds are ubiquitous at all scales in the metasediments, but the large folds shown in the section are highly hypothetical. However, there are some clues to support the assumption of large-scale, north-verging, km-size folds. Firstly, a very specific horizon of Mg-chloritoid and margarite schists is known close to the top of the upper slab near Bonneval, and similar rocks outcrop in a large metasedimentary lens above Ceresole, in-between the two slabs. Such „silvery micaschists" may either represent metabauxites, or result from deformation and metasomatism (Bertrand, 1968; Chopin, 1979; Dal Piaz and Lombardo, 1986; Ballèvre, 1988; Delle Piane et al., 2002). Secondly, greenstones and eclogites are mostly developed above the upper orthogneiss slab (upper Vallegrande), and further occurrences are mentioned in-between the two main orthogneiss slabs (e.g. Telessio, cited by Dal Piaz and Lombardo, 1986).

2.2. Age of pre-Alpine formations in the Internal Crystalline Massifs

Piemonte basement domes

The age of the GP orthogneisses in the Orco valley near Ceresole (Fig. 1) was estimated around 340–350 Ma in using the total lead method on zircon (Pangaud et al., 1957; Buchs et al., 1962; Chessex et al., 1964). Permian zircon U–Pb ages were recently found (Bertrand et al., 2000b) for orthogneisses from the western part of the GP massif at L'Ecot (Fig. 1): magmatic overgrowths, dated at 269 ± 6 Ma (porphyritic meta-granite), and 263 ± 36 Ma (dark enclave), with inherited cores at ca. 2 Ga and ca. 600 Ma.

The other Piemonte gneiss domes (DM and MR, Fig.1), show a larger variety of rock-types (Bearth, 1952; Vialon, 1966). In DM, an onion-shaped stack of tectonic sheets, the lowermost tectonic unit (Pinerolo formation) is considered to be a high-pressure equivalent of the Briançonnais Upper Carboniferous coal measures. Coal beds are replaced by massive graphite, and meta-dioritic dykes crosscut a meta-arkose-conglomerate-graphite trilogy, very similar to the cyclothems of the low-grade „Zone Houillère Briançonnaise" (ZH on Fig. 1). DM has yielded an Ordovician age at 457 ± 2 Ma (Punta Muret) whilst most orthogneisses are younger, with ages of 304 ± 3 Ma, 290 ± 2 and 288 ± 2 Ma, and three poorly constrained ages around 275 Ma (Bussy and Cadoppi, 1996; Gebauer et al., 1997; Paquette et al., 1999). In MR, metapelites yielded 330 Ma-old ages on monazites included in large garnets, while matrix monazites (in equilibrium with low-pressure high-grade minerals) were attributed to Permian plutonic activity (Engi et al., 2001). There, monazites at ca. 270 Ma (Engi et al., 2001) and a SHRIMP zircon age at 272 Ma (Liati et al., 2001)

confirm previous age determinations (Köppel and Grünenfelder, 1975).

Austro-Alpine and Apulian basements

In the Sesia zone and Dent Blanche massifs several Permian intrusives have been dated: Monte Mucrone metagranite at 286 ± 2 (Paquette et al., 1989) and 293+1/–2 (Bussy et al., 1998); Monte Emilius orthogneiss at 293 ± 3, Arolla orthogneiss at 289 ± 2, Sermenza gabbro at 288+2/–3 (Bussy et al., 1998); Mont Collon gabbro at 284.2 ± 0.7 and 282.9 ± 0.6 Ma (Monjoie et al., 2002); several eclogite zircon cores yielded ages at ca. 285 Ma, and also a leucocratic dyke crosscutting the 350 Ma old Cima di Bonze metagabbro (Rubatto, 1998). The Ivrea Zone exhibits a famous mantle-crust transition where associated plutons yielded Late Carboniferous to Triassic ages on zircon and monazite (Vavra et al., 1999 and refs. therein), while other studies suggest a lower Paleozoic event (Pin, 1990). As a whole, the Permian period in the Apulian realm appears as a period of post-orogenic crustal growth by magmatic underplating, synchronous with Permian volcanism and plutonism in the Southern Alps (D'Amico and Rottura, 1982), and with a thermal metamorphism in the Austro-Alpine realm (Schuster et al., 2004).

Briançonnais - Grand-Saint-Bernard basements

Most dating studies of metagranites in GSB have yielded lower Paleozoic ages (Guillot et al., 1991; Bussy et al., 1996a; Bertrand and Leterrier, 1997; Bertrand et al., 2000a; Bertrand et al., 2000b; Guillot et al., 2002). A large Upper Carboniferous to Permian basin, initiated in Visean to Lower Namurian times, follows the whole arc of the Western Alps (ZH on Fig. 1). Sediments deposited in the 325–300 Ma age range are widespread in the Briançonnais domain and typically show no pre-Alpine metamorphism, hence Variscan metamorphic ages have rarely been found, and there are few Variscan granitoids dated up to now. Exceptions are the Costa Citrin granite in Aosta Valley (323 ± 8 Ma and 324 ± 17 Ma; Bertrand et al., 1998) and the Cogne diorite-granodiorite pluton of calc-alkaline to subalkaline affinity, dated at ca. 356 ± 3 Ma (loc. on Fig. 1; Bertrand et al., 2000b). Permian ages have been also found in equivalent units of the Central Alps (Tambo 268 ± 0.4 Ma, Suretta 268.3 ± 0.6 Ma; Marquer et al., 1998) and in GSB (269 ± 2 Ma for the Randa orthogneiss; Bussy et al., 1996).

In the GSB domain, the only trace of the widespread 330-340 Ma granitoids and associated metamorphism of the Variscan belt is yielded by a monazite age from the Grand Saint Bernard area (Giorgis et al., 1999). The resulting impression is that the Variscan metamorphism was either absent or of very low grade in a large part of the GSB. So, while the Mont Blanc and Velay granites intruded at ca. 300 Ma in the ECM and the Eastern French Central Massif, clastic deposition and coal measures were dominating the Briançonnais landscape.

2.3. Sampling

The choice of the GP sample locations was guided by structural depth rather than by distribution in map view (Figs. 1 and 2). Contrasted textural types and local environments were selected: (i) metagranites from the lower orthogneiss slab, comparable to our previous samples at l'Ecot in the upper slab, and (ii) metavolcanics associated with the metasediments. Two unsuccessful attempts were made to use samples of the Erfaulet metagranite, at the deepest level of the Money window, which did not yield enough zircon for analysis.

Gran Paradiso orthogneisses

ZH 00 05 was sampled in the Orco valley (near Noasca) from the structurally deepest part of the Gran Paradiso massif (Fig. 2). It is a coarse-grained, weakly deformed porphyritic granite that comprises quartz, K-feldspar megacrysts (perthitic orthoclase and microcline), albite, phengite, small stubby grains of zoisite, and large, broken and retrogressed garnet (pre- or early Alpine?). Magmatic biotite is still recognisable though it was largely replaced by metamorphic biotite, phengite and titanite. As in the other samples, the small number of zircon grains observed in thin sections precludes any reliable estimate of preferential relationship with other minerals.

ZH 00 06 is a medium-grained porphyritic granite dyke cross-cutting the banding of metasediments. It was sampled on the eastern buttress of the Telessio Dam, close to the place where sillimanite (replaced by Alpine kyanite) has been identified in the metasediments and interpreted to result from pre-Alpine contact metamorphism (Compagnoni and Prato, 1969). Old biotite is completely replaced by new biotite + phengite + titanite. Plagioclase is replaced by albite + epidote + zoisite. Garnet porphyroclasts occur in complex association with quartz and many tiny euhedral garnet grains.

ZH 00 14 and ZH 00 15 are two porphyritic granites from the eastern bank of the Telessio lake; they are closely associated and form a magmatic breccia (Callegari et al., 1969). The apparently older rock type (ZH 00 14) is light in colour and slightly deformed, whilst the younger one, the

matrix of the breccia, is grey and shows a magmatic fluidal texture (ZH 00 15). ZH 00 14 is composed of quartz and large perthitic K-feldspar grains with superimposed euhedral albite. Garnet porphyroclasts are partially replaced by chlorite upon retrogression. Magmatic biotite is replaced by white mica and newly crystallised small biotite. The grey granite (ZH 00 15) shows recrystallised quartz and albite in small grains. Large perthitic K-feldspar is invaded by quartz and albite. Large garnet grains are retrogressed, and many small euhedral garnet crystals occur in the recrystallised matrix.

Metavolcanic rocks

ZH 98 14 is a presumed metarhyolite from the „Bonneval series" at Piedmontet. It is a pale green albite-phengite gneiss in which embayed quartz has occasionally been observed, suggesting a rhyolitic origin.

ZH 00 13 is a homogeneous albite-bearing gneiss from Piano delle Agnelere near Bivacco Carpano. It is a grey to brown, medium-grained gneiss. The rock is an albite-bearing gneiss, K-feldspar free, with abundant quartz associated with biotite, phengite, garnet, clinozoisite, zoisite, and titanite. The several decametre-thick gneiss unit is interlayered with metasediments, which suggests that this rock-type may be derived from a volcano-clastic rock predating the main Gran Paradiso orthogneiss.

3. Geochronology

3.1. Analytical procedures

Two complementary approaches were used: isotope dilution – thermo-ionic mass spectrometry (IDTIMS) and sensitive high-resolution ion microprobe (SHRIMP). For the IDTIMS technique only tiny zircon needles containing occasional magmatic inclusions were used. Inclusions were identified by their shape (high magnification microscopy) and from back-scattered SEM observation. Analysed needles were 100 μm long on average, with a thickness and width <10 μm. The average mass of single needles was 1–2 μg for sample ZH 0013 and in the range 3–7 μg for samples ZH 0005 and ZH 0015. The number of analysed needles for each sample is indicated in Table 1. Stubby prisms (100–150 μm in size) were selected for ion probe dating because preliminary SEM investigations had shown that zoned magmatic overgrowths were present around inherited cores. Analyses of magmatic overgrowths were preferred in this study because numerous core analyses had been carried out during the previous study that gave a good estimate of the inheritance ages (Bertrand et al., 2000b).

Isotope dilution (IDTIMS) – After zircon selection, sample dissolution, chemical preparation and mass spectrometry were performed according to improved, miniaturized techniques (Paquette and Pin, 2001). Total blanks were 10–15 pg for Pb and less than 1 pg for U during the analytical period. The U–Pb isotopic results were performed on a VG Sector 54-30 mass spectrometer (Clermont-Ferrand) in a multi-collector static mode and ^{204}Pb was simultaneously measured with a Daly detector ion-counting system. Individual fraction ellipse errors (2σ) were determined and regression calculations performed using the PbDat 1.24 and Isoplot/Ex 2.49 programs respectively (Ludwig, 2000). Age uncertainties are quoted at the 2σ level. The decay constants used for the U–Pb system are those recommended by the IUGS (Jaffey et al., 1971; Steiger and Jäger, 1977). Results are shown in Table 1 and Fig. 5.

SHRIMP dating – Zircons were analysed at the Australian National University using the SHRIMP II and the usual data reduction (Compston et al., 1992; Williams and Claesson, 1987). Measured U/Pb ratios were normalised to a $^{206}Pb/^{238}U$ value corresponding to the 416.8 ± 1.1 age of the Temora 1 standard (Black et al., 2003). U and Th concentrations were determined using the same standard. Corrections for common Pb were made using the measured $^{204}Pb/^{206}Pb$ ratios and the relevant model Pb compositions (Cumming and Richards, 1975). Uncertainties in the isotopic ratios and ages in the data table (and in the error ellipses on the figures) are reported at the 1σ level, but final pooled ages are reported as weighted means at the 95% confidence level. All age calculations and statistical assessment of the data have been done using the geochronological statistical software package Isoplot/Ex 2.49 (Ludwig, 2000). Results are shown on Table 2 and Fig. 5.

3.2. Results

Gran Paradiso orthogneisses

ZH 00 05 – Zircon grains are euhedral, and their morphological types (Pupin, 1980) show a typical calc-alkaline to anatectic trend with dominant S6-S12-S17 types (Fig. 3). Back-scattered SEM images do not show any evidence of Alpine overgrowth, but a regular magmatic envelope surrounds inherited cloudy cores. IDTIMS results from this sample are not quite concordant (Fig. 5). The discordant analytical point being close, the discordia line (3 fractions) yields imprecise intercepts at –75 ± 1500 and 275 ± 25 Ma (MSWD =

Table 1 Isotope dilution and thermal ionisation mass spectrometry (IDTIMS) analytical data.

Sample	Weight	Nb of	Concentrations			Atomic ratios						Apparent ages				
		grains	U	common Pb	Pb Tot	$^{206}Pb/^{204}Pb$	$^{206*}Pb/^{238}U$		$^{207*}Pb/^{235}U$		$^{207*}Pb/^{206*}Pb$	206/238	207/235	207/206	Error	Pb blank
	mg		ppm	ppm	ppm		a)	2σ%	a)	2σ%	a)	2σ%				corr.	pg
ZH05-1	0.033	5	736	0.12	30	4283	0.04266	0.22	0.30459	0.39	0.05179	0.31	269.3	270	276±7.1	0.6	11
ZH05-2	0.033	9	587	0.16	24	3128	0.04242	0.3	0.30314	0.52	0.05183	0.41	267.8	268.8	277.7±9.3	0.62	11
ZH05-3	0.009	9	1673	0.89	70	1736	0.04214	0.44	0.3009	0.84	0.05178	0.69	266	267	275.9±16	0.58	15
ZH13-1	0.012	10	2652	10.6	116.7	625	0.04202	0.18	0.30015	0.32	0.0518	0.25	265.3	266.5	276.8±5.7	0.61	11
ZH13-2	0.018	13	1501	2.03	66.6	1419	0.04259	0.26	0.30403	0.48	0.05178	0.39	268.9	269.5	275.5±8.8	0.59	15
ZH13-3	0.017	15	1676	2.14	73.6	1508	0.04284	0.24	0.30638	0.45	0.05187	0.36	270.4	271.4	279.6±8.2	0.59	15
ZH13-4	0.024	13	1278	0.9	51	2202	0.04178	0.24	0.29847	0.43	0.05181	0.34	263.9	265.2	277.1±7.9	0.6	15
ZH15-1	0.043	12	950	0.22	39	5264	0.04243	0.16	0.3024	0.25	0.05169	0.19	267.9	268.3	271.8±4.3	0.67	11
ZH15-2	0.025	9	873	0.33	35.4	3002	0.04267	0.23	0.30467	0.43	0.05178	0.35	269.4	270	275.7±7.9	0.59	11
ZH15-3	0.056	20	849.6	1.81	36	1106	0.04226	0.22	0.30149	0.32	0.05174	0.23	266.8	267.6	273.9±5.2	0.72	15

a) corrected for fractionation. spike. blank and common lead (Stacey and Kramers, 1975). All calculations done with Pbdat (Ludwig, 2000).

Fig. 3 Microscope and SEM (back-scatter mode) images of zircon grains analysed by TIMS. Possible magmatic inclusions may be observed (05 b, c; 13 b; 15 b, c). SEM images show only magmatic zoning (13 e), inherited cores (15 d), or complexly zoned stubby grains (not analysed).

0.08) so we chose to use the weighted average of $^{207}Pb/^{206}Pb$ ages that yields **277 ± 5** Ma (2σ). This age is interpreted as the best estimate for the crystallisation age.

ZH 00 06 – Separated zircons are sometimes rounded and cloudy, but many grains are perfectly clear and show magmatic inclusions. SEM and CL images show inherited cores and external magmatic zoning (Fig. 4). Zircon typology (Pupin, 1980) indicates a calc-alkaline to sub-alkaline tendency (S7 and S2 dominant). SHRIMP results do not show a coherent grouping for the almost concordant $^{206}Pb/^{238}U$ ages, probably because the primary beam was low and unstable during these analyses. However, if we exclude the obviously inherited points (7, 8, 9), a discordia line (Fig. 5) indicates an upper intercept $^{207}Pb/^{206}Pb$ age of **273 ± 36 Ma** (MSWD = 0.52). The corresponding lower

Table 2A Summary of SHRIMP U-Pb zircon data for sample **ZH 00 06.**

Grain Spot	locus	$^{206}Pb_c$ %	U ppm	Th ppm	$^{232}Th/^{238}U$	$^{206}Pb^*$ ppm	(1) $^{206}Pb/^{238}U$ Age	(2) $^{206}Pb/^{238}U$ Age	(1) $^{207}Pb/^{206}Pb$ Age	% Disc.	Total $^{238}U/^{206}Pb$	±%	Total $^{207}Pb/^{206}Pb$	±%	(1) $^{207}Pb^*/^{206}Pb^*$	±%	(1) $^{207}Pb^*/^{235}U$	±%	(1) $^{206}Pb^*/^{238}U$	±%	error corr.
1.1	tip	0.05	339	55	0.17	10.5	227.8 ± 4.7	227.7 ± 4.8	245 ± 54	7	27.80	2.1	0.0511	2.4	0.0511	2.4	0.2534	3.2	0.036	2.1	0.66
2.1	tip	0.00	1544	64	0.04	52.5	250.3 ± 2.5	250.6 ± 2.5	205 ± 51	-22	25.26	1.0	0.0502	2.2	0.0502	2.2	0.2741	2.4	0.0396	1.0	0.42
3.1	tip	0.31	1598	59	0.04	33.0	153.0 ± 1.8	152.6 ± 1.9	265 ± 86	42	41.62	1.2	0.0515	3.7	0.0515	3.7	0.1707	3.9	0.0240	1.2	0.31
4.1	tip	0.05	2200	82	0.04	76.2	254.7 ± 2.4	254.5 ± 2.4	274 ± 22	7	24.82	0.96	0.0517	0.95	0.0517	0.95	0.2874	1.3	0.0403	0.96	0.71
4.2	ct	0.07	226	45	0.21	7.75	252.1 ± 4.2	251.9 ± 4.2	278 ± 66	9	25.08	1.7	0.0518	2.9	0.0518	2.9	0.2850	3.4	0.0399	1.7	0.5
5.1	ct	0.24	220	161	0.75	7.89	263.7 ± 5.4	263.1 ± 5.4	347 ± 83	24	23.95	2.1	0.0534	3.7	0.0534	3.7	0.307	4.2	0.0417	2.1	0.49
6.1	ct	0.00	336	100	0.31	11.9	260.4 ± 2.9	260.6 ± 2.9	232 ± 52	-12	24.26	1.1	0.0508	2.3	0.0508	2.3	0.2887	2.5	0.0412	1.1	0.45
7.1	ct	0.07	177	115	0.67	7.22	298.5 ± 4.1	298.3 ± 4.2	321 ± 76	7	21.10	1.4	0.0528	3.3	0.0528	3.3	0.345	3.6	0.0474	1.4	0.39
8.1	tip	0.19	468	52	0.11	17.9	280.1 ± 2.8	279.6 ± 2.8	346 ± 37	19	22.51	1.0	0.0534	1.6	0.0534	1.6	0.3270	1.9	0.0444	1.0	0.53
9.1	tip	0.00	398	30	0.08	23.7	431.4 ± 4.0	432.3 ± 4.1	357 ± 32	-21	14.45	0.96	0.0537	1.4	0.0537	1.4	0.5120	1.7	0.0692	0.96	0.57
10.1	tip	0.00	403	41	0.10	15.1	274.4 ± 2.8	274.6 ± 2.9	252 ± 41	-9	22.99	1.0	0.0512	1.8	0.0512	1.8	0.3073	2.1	0.0435	1.0	0.51
12.1	tip	0.04	472	41	0.09	17.3	269.9 ± 2.8	269.8 ± 2.8	283 ± 45	5	23.39	1.1	0.0519	2.0	0.0519	2.0	0.3062	2.2	0.0428	1.1	0.47
12.2	ct	0.14	214	68	0.33	7.55	258.8 ± 3.9	258.4 ± 4.0	308 ± 70	16	24.41	1.5	0.0525	3.1	0.0525	3.1	0.297	3.4	0.041	1.5	0.45
13.1	tip	0.09	852	55	0.07	31.5	271.2 ± 2.5	271.0 ± 2.6	304 ± 35	11	23.27	0.95	0.0524	1.5	0.0524	1.5	0.3106	1.8	0.043	0.95	0.53

Error in Standard calibration was 0.37% (not included in above errors but required when comparing data from different mounts). ct = centre of grain

Table 2B Summary of SHRIMP U-Pb data for zircons from sample **ZH 00 14**.

Grain Spot	locus	$^{206}Pb_c$ %	U ppm	Th ppm	$^{232}Th/^{238}U$	$^{206}Pb^*$ ppm	(1) $^{206}Pb/^{238}U$ Age	(2) $^{206}Pb/^{238}U$ Age	(1) $^{207}Pb/^{206}Pb$ Age	% Disc.	Total $^{238}U/^{206}Pb$	±%	Total $^{207}Pb/^{206}Pb$	±%	(1) $^{207}Pb^*/^{206}Pb^*$	±%	(1) $^{207}Pb^*/^{235}U$	±%	(1) $^{206}Pb^*/^{238}U$	±%	error corr.
1.1	tip	0.10	442	38	0.09	17.0	282.6 ± 3.1	282.4 ± 3.2	316 ± 51	11	22.31	1.1	0.0527	2.2	0.0527	2.2	0.3257	2.5	0.0448	1.1	0.45
2.1	tip	0.24	578	85	0.15	20.3	257.4 ± 1.9	257.3 ± 1.9	272 ± 59	5	24.50	0.73	0.0533	1.9	0.0517	2.6	0.2904	2.7	0.0407	0.74	0.27
3.1	tip	0.00	630	47	0.08	24.0	279.0 ± 2.1	279.1 ± 2.1	266 ± 43	-5	22.61	0.76	0.0515	1.9	0.0515	1.9	0.3144	2.0	0.0442	0.76	0.38
4.1	tip	0.24	396	83	0.22	14.6	271.5 ± 2.4	270.9 ± 2.4	355 ± 54	24	23.24	0.90	0.0536	2.4	0.0536	2.4	0.3180	2.5	0.0430	0.90	0.35
5.1	tip	0.00	698	116	0.17	26.9	282.6 ± 1.9	282.7 ± 1.9	265 ± 42	-7	22.32	0.67	0.0515	1.8	0.0515	1.8	0.3184	1.9	0.0448	0.67	0.35
6.1	ct	0.18	256	55	0.22	9.57	275.1 ± 3.8	274.6 ± 3.8	337 ± 69	18	22.94	1.4	0.0532	3.0	0.0532	3.0	0.320	3.3	0.0436	1.4	0.42
6.2	?	0.21	985	104	0.11	35.4	264.0 ± 1.6	263.4 ± 1.6	337 ± 37	22	23.92	0.62	0.0532	1.6	0.0532	1.6	0.3066	1.8	0.0418	0.62	0.35
7.1	tip	0.04	922	100	0.11	35.3	281.4 ± 1.7	281.3 ± 1.8	294 ± 37	4	22.41	0.63	0.0522	1.6	0.0522	1.6	0.3211	1.7	0.0446	0.63	0.36
8.1	ct	0.30	803	321	0.41	29.6	271.2 ± 1.8	270.4 ± 1.9	375 ± 48	28	23.27	0.68	0.0541	2.1	0.0541	2.1	0.3205	2.2	0.043	0.68	0.30
9.1	ct	0.54	102	82	0.83	8.62	604.0 ± 8.9	600.9 ± 9.1	752 ± 65	20	10.18	1.5	0.0643	3.1	0.0643	3.1	0.871	3.4	0.0982	1.5	0.45
10.1	ct	0.00	202	48	0.25	7.89	286.7 ± 3.8	287.1 ± 3.9	242 ± 84	-18	21.98	1.3	0.0510	3.7	0.0510	3.7	0.320	3.9	0.0455	1.3	0.34
11.1	tip	0.21	204	61	0.31	7.15	257.9 ± 3.5	257.3 ± 3.7	330±150	22	24.50	1.4	0.0530	6.5	0.0530	6.5	0.298	6.7	0.0408	1.4	0.21
12.1	ct	0.36	211	47	0.23	12.1	415.7 ± 4.9	414.3 ± 5.0	527 ± 61	21	15.01	1.2	0.0579	2.8	0.0579	2.8	0.532	3.0	0.0666	1.2	0.40
13.1	tip	0.08	744	61	0.08	27.6	272.3 ± 2.0	272.1 ± 2.1	299 ± 65	9	23.18	0.76	0.0523	2.8	0.0523	2.8	0.3112	2.9	0.0431	0.76	0.26
14.1	tip	0.15	1261	111	0.09	47.9	278.8 ± 2.3	278.4 ± 2.3	332 ± 35	16	22.62	0.83	0.0531	1.5	0.0531	1.5	0.3235	1.7	0.0442	0.83	0.48
14.2	ct	0.22	661	378	0.59	24.2	269.1 ± 3.5	268.5 ± 3.5	345 ± 47	22	23.46	1.3	0.0534	2.1	0.0534	2.1	0.3137	2.5	0.0426	1.3	0.53
15.1	ct	1.34	772	63	0.08	207	1.75±21	1.73±23	1.92± 13	9	3.200	1.4	0.1177	0.70	0.1177	0.70	5.072	1.5	0.3125	1.4	0.89
15.2	tip	0.19	517	57	0.11	18.8	267.4 ± 2.5	266.9 ± 2.6	333 ± 58	20	23.61	0.96	0.0531	2.5	0.0531	2.5	0.3101	2.7	0.0423	0.96	0.35
16.1	tip	0.28	509	65	0.13	18.7	269.7 ± 2.5	268.9 ± 2.6	365 ± 56	26	23.41	0.95	0.0539	2.5	0.0539	2.5	0.3172	2.6	0.0427	0.95	0.36
17.1	tip	0.00	556	101	0.19	20.9	275.8 ± 2.5	276.4 ± 2.5	200 ± 57	-38	22.87	0.92	0.0501	2.5	0.0501	2.5	0.3020	2.6	0.0437	0.92	0.35

Error in Standard calibration was 0.37% (not included in above errors but required when comparing data from different mounts). ct = centre of grain

Table 2C Summary of SHRIMP U-Pb zircon data for sample **ZH 98 14.**

Grain Spot	locus	$^{206}Pb_c$ %	U ppm	Th ppm	$^{232}Th/^{238}U$	$^{206}Pb^*$ ppm	(1) $^{206}Pb/^{238}U$ Age	(2) $^{206}Pb/^{238}U$ Age	(1) $^{207}Pb/^{206}Pb$ Age	% Disc.	Total $^{238}U/^{206}Pb$	± %	Total $^{207}Pb/^{206}Pb$	± %	(1) $^{207}Pb^*/^{206}Pb^*$	± %	(1) $^{207}Pb^*/^{235}U$	± %	(1) $^{206}Pb^*/^{238}U$	± %	error corr.
3.3	edg	0.10	827	72	0.09	30.9	274.3 ± 2.2	274.1 ± 2.2	310 ± 24	12	22.98	0.80	0.0533	0.78	0.0525	1.0	0.3150	1.3	0.0435	0.80	0.61
7.2	tip	0.12	1400	128	0.09	51.5	270.0 ± 2.1	270.0 ± 2.1	271 ± 19	0	23.35	0.80	0.0527	0.58	0.0517	0.85	0.3047	1.2	0.0428	0.80	0.69
10.1	tip	0.16	1329	542	0.42	47.6	262.9 ± 2.4	262.9 ± 2.4	266 ± 22	1	23.98	0.92	0.0529	0.64	0.0516	0.97	0.2960	1.3	0.0416	0.92	0.69
11.1	tip	0.12	907	248	0.28	31.9	258.1 ± 2.0	258.0 ± 2.0	279 ± 34	7	24.45	0.78	0.0528	0.88	0.0519	1.5	0.2922	1.7	0.0409	0.79	0.47
11.1	ct	0.14	1095	406	0.38	40.2	269.2 ± 2.0	268.9 ± 2.1	300 ± 32	10	23.42	0.78	0.0535	1.1	0.0523	1.4	0.3076	1.6	0.0426	0.78	0.48
12.1	edg	0.32	800	172	0.22	29.3	268.5 ± 2.1	268.6 ± 2.1	261 ± 40	-3	23.44	0.80	0.054	0.78	0.0514	1.7	0.3017	1.9	0.0425	0.81	0.42
13.1	edg	0.12	2179	151	0.07	73.0	246.2 ± 1.8	246.0 ± 1.8	269 ± 19	8	25.66	0.76	0.0526	0.50	0.0516	0.82	0.2770	1.1	0.0389	0.76	0.68
14.1	tip	0.10	1876	98	0.05	68.7	268.8 ± 2.0	269.0 ± 2.0	241 ± 16	-12	23.46	0.75	0.0518	0.52	0.0510	0.69	0.2995	1.0	0.0426	0.75	0.74
15.1	ct	0.12	1258	66	0.05	44.6	260.2 ± 2.0	259.9 ± 2.0	301 ± 24	14	24.25	0.78	0.0533	0.67	0.0523	1.1	0.2973	1.3	0.0412	0.79	0.59
16.1	ct	0.08	972	439	0.47	38.5	290.3 ± 2.2	290.3 ± 2.2	285 ± 22	-2	21.69	0.78	0.0527	0.72	0.052	0.96	0.3302	1.2	0.0461	0.78	0.63
16.2	ct	0.09	874	302	0.36	33.6	282.0 ± 2.2	282.1 ± 2.2	271 ± 19	-4	22.34	0.78	0.0524	0.74	0.0517	0.82	0.3186	1.1	0.0447	0.78	0.69
17.1	ct	0.20	706	88	0.13	25.1	260.4 ± 2.1	260.7 ± 2.1	224 ± 46	-16	24.21	0.82	0.0522	1.0	0.0506	2.0	0.2877	2.2	0.0412	0.82	0.38
18.1	tip	0.55	590	291	0.51	18.8	234.0 ± 2.0	233.6 ± 2.0	282 ± 57	17	26.91	0.84	0.0563	0.99	0.0519	2.5	0.2646	2.6	0.034	0.85	0.32
19.1	tip	0.16	1310	77	0.06	49.1	274.9 ± 2.1	275.0 ± 2.1	255 ± 22	-8	22.92	0.76	0.0526	0.62	0.0513	0.96	0.3082	1.2	0.0436	0.77	0.62
20.1	tip	0.52	2153	145	0.07	62.6	213.5 ± 1.6	213.2 ± 1.6	256 ± 68	17	29.54	0.76	0.0555	1.6	0.0513	2.9	0.2384	3.0	0.0337	0.77	0.25
21.1	tip	0.21	2874	165	0.06	77.8	199.6 ± 1.8	199.5 ± 1.8	223 ± 25	10	31.73	0.89	0.0523	0.57	0.0506	1.1	0.2195	1.4	0.0314	0.89	0.64
22.1	tip	0.12	1081	144	0.14	40.2	272.6 ± 2.2	272.7 ± 2.2	261 ± 24	-4	23.12	0.83	0.0526	0.69	0.0514	1.0	0.3064	1.3	0.0432	0.83	0.62

Error in Standard calibration was 0.37% (not included in above errors but required when comparing data from different mounts). ct = centre of grain

(1) Errors are 1-sigma; Pb_c and Pb^* indicate respectively the common and radiogenic portions, respectively. Errors correlation is given in the last column.
(2) Common Pb corrected by assuming $^{206}Pb/^{238}U$-$^{207}Pb/^{235}U$ age-concordance.

Fig. 4 Cathodoluminescence images of zircon grains analysed by SHRIMP showing the prevalence of regularly zoned edges and tips over more or less complex inherited cores (quoted as centres in Table 2).

intercept is at 46 ± 220 Ma. Concerning $^{206}Pb/^{238}U$ ages, the grouping is not good: 8 points indicate a weighted average of **264 ± 7 Ma** (MSWD = 7.4). Due to the problems during analysis, the $^{206}Pb/^{238}U$ weighted average of 264 Ma is imprecise; it is interpreted as a minimum estimate of the crystallisation age.

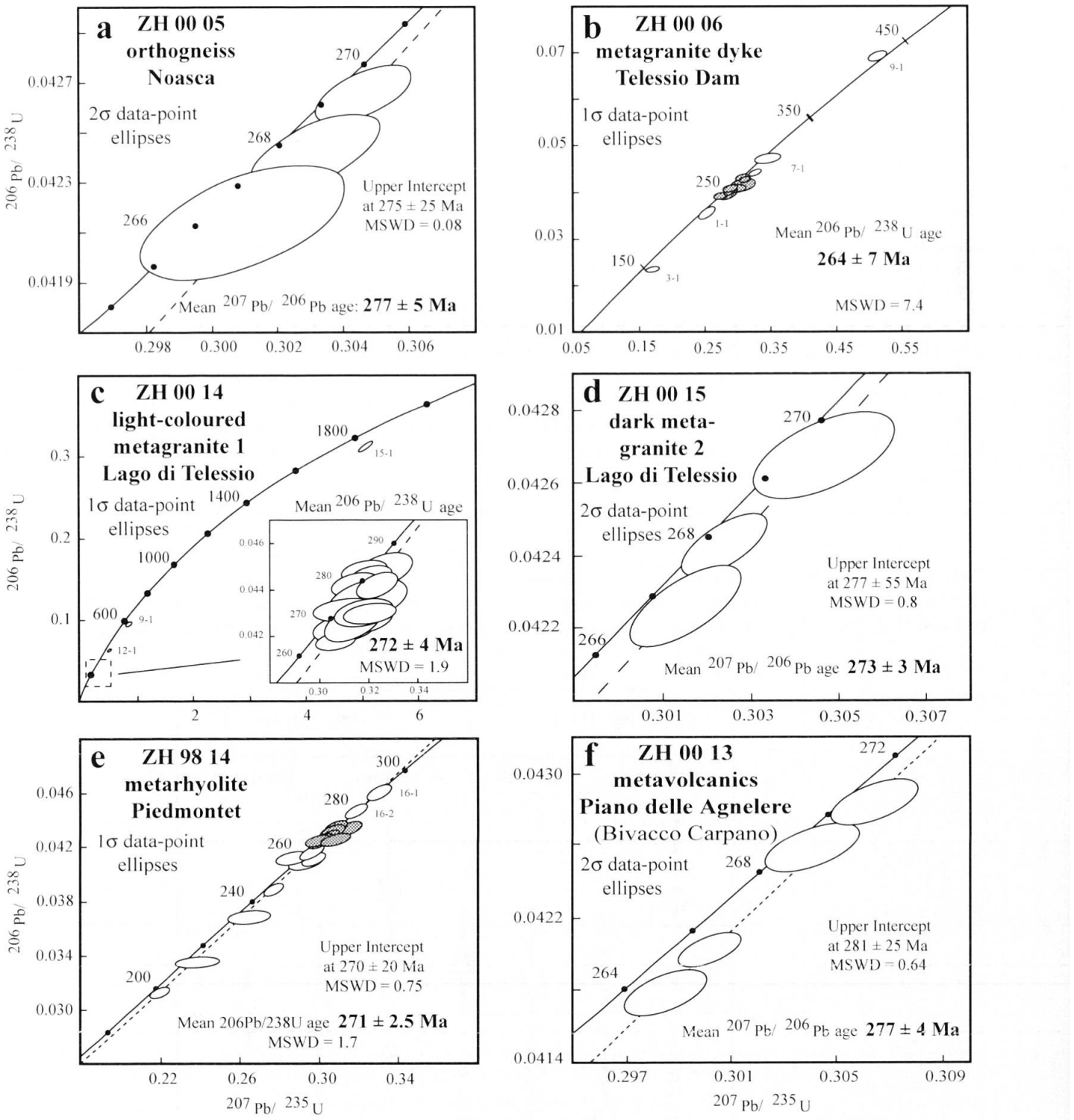

Fig. 5 SHRIMP and TIMS diagrams: (a) TIMS concordia diagram, Noasca orthogneiss (ZH0005); (b) SHRIMP concordia diagram, Telessio dam granite dyke (ZH0006); (c) SHRIMP concordia diagram, Lago di Telessio, light granite of breccia blocks (ZH0014) with enlargement of the pooled analytical points; (d) TIMS concordia diagram, Lago di Telessio, grey granite of breccia matrix (ZH0015); (e) SHRIMP concordia diagram, Piedmontet metarhyolite (ZH9814); (f) TIMS concordia diagram, Piano delle Agnelere, metavolcanite (ZH0013).

ZH 00 14 – Zircons are euhedral, often rich in inclusions and show a calc-alkaline typology (S2, S7, S12, S17 types are dominant). SEM and CL images show inherited cores and external magmatic zoning (Fig. 4). Twenty points were analysed using SHRIMP on magmatic zoned domains and cores from sample ZH 00 14 (Fig. 5). Three cores (12-1, 9-1 and 15-1) are clearly inherited and correspond respectively to ages of ca. 400, 600 and 1900 Ma. The seventeen remaining points are grouped and almost concordant, they define a $^{206}Pb/^{238}U$ age (weighted average) of **272 ± 4 Ma**

(MSWD = 1.9 at 95% confidence level). On a Tera-Wasserburg plot (not shown) drawn with ratios uncorrected for common lead, the seventeen points are aligned with a lower intercept at 284 ± 10 Ma, interpreted to indicate a maximum age for the crystallisation of zircon.

ZH 00 15 – Zircon occurs as stubby prisms and thin needles (Fig. 3). The main types are S6 and S12, usually attributed to a calc-alkaline trend, but some grains (S10-S15) are close to a sub-alkaline tendency and may represent inherited grains. IDTIMS results for sample ZH 00 15 (Fig. 5) concern three discordant fractions of tiny needles. The points are aligned but too close to correctly define a discordia line (calculated intercepts are: 118 ± 910 Ma and 277 ± 55 Ma; MSWD = 0.8). The points being close to the Concordia, the weighted average $^{207}Pb/^{206}Pb$ age of **273 ± 3 Ma** (2σ) is considered as a good estimate for the age of the last crystallised magmatic zircons.

Metavolcanic rocks

ZH 98 14 – Zircon types are dominantly alkaline (P3 to P1) but some L types (with dominant 211 pyramid) imply some anatectic contamination. SHRIMP results include 17 points, aligned on a discordia line (Fig. 5) with an upper intercept at 270 ± 20 Ma (MSWD = 0.75). Two points (16-1, 16-2) are slightly above the intercept and may correspond to an inheritance, as confirmed by their location on a Tera-Wasserburg diagram with a lower intercept at 272 ± 12 Ma (not shown). A group of 7 points is clustered on the concordia and the corresponding weighted mean of $^{206}Pb/^{238}U$ age is **271.0 ± 2.5 Ma** (MSWD = 1.7 at 95% confidence level) regarded as the best estimate of the crystallisation age.

ZH 00 13 – The zircon population is complex and includes slightly rounded shapes suggesting xenocrysts or metamorphic grains. However, the ubiquity of magmatic regular zoning observed on SEM images and especially the presence of thin euhedral needles with magmatic inclusions suggest a partly magmatic origin for that rock (Fig. 3). From Pupin's typology (Pupin, 1980), most grains are located on a calc-alkaline trend (S13 dominant), though they are mixed with grains from a sub-alkaline source (inheritance). Furthermore, inherited cores are obvious on SEM back-scattered images of stubby prisms. In order to esti-

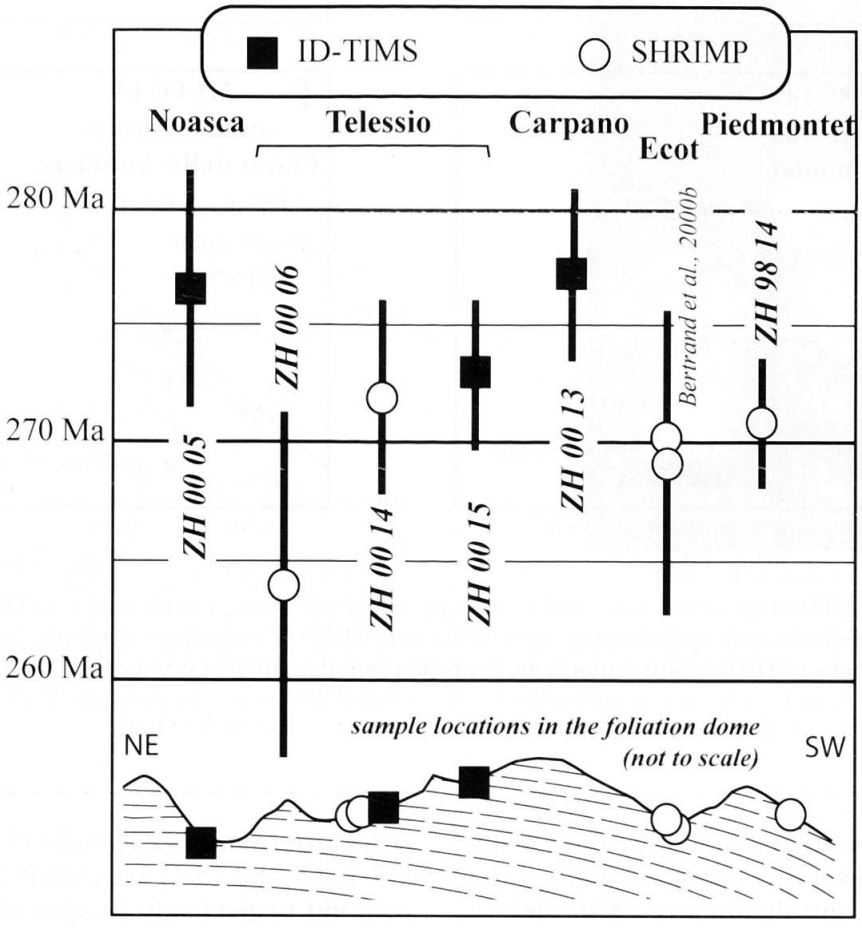

Fig. 6 A synthesis of U–Pb ages from the Gran Paradiso. Note that the data for ZH 00 06 represent a minimum age. Recently, two comparable zircon U–Pb SHRIMP ages were published (Ring et al., 2005) from porphyritic orthogneiss samples located at the NE end of this section (270.2 ± 5 Ma) and near its centre (269 ± 6.5 Ma).

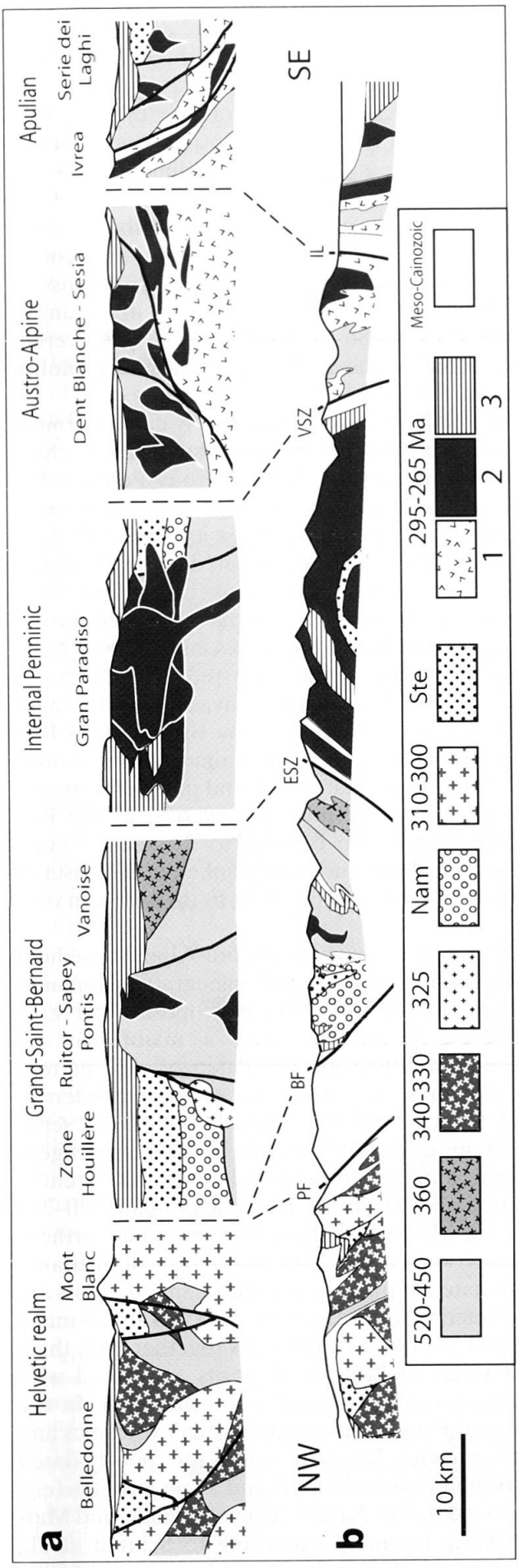

Fig. 7 Paleozoic units in Western Alps. (a): reconstitution of late Permian sections for five W-Alpine zones from available age data (without scale) - (b): present-day sketch section of the W-Alps. - The present-day profile (b) was drawn after Schmid and Kissling (2000), their interpretative parts toward depth were omitted. The age distribution in the Ivrea lower crust was derived from age data by Pin (1990). The Gran Paradiso gross structure in (b) is adapted from Compagnoni et al. (1974) and Le Bayon and Ballèvre (2004). Blank spaces have been chosen for the following reasons: (PF) major Paleo-Meso-Cainozoic paleogeographic differences between the Helvetic and Grand-Saint-Bernard domains; (ESZ) Alpine metamorphic gap from ~ 0.5 GPa in Grand-Saint-Bernard up to ⩾ 2 GPa in the Gran Paradiso; (VSZ) time-gap between the ~ 35-45 Ma Gran Paradiso HP-metamorphism and the ~ 65-76 Ma Sesia HP-metamorphism; (IL) metamorphic gap across the Insubric Line, with no Alpine metamorphism to the East. - Key to symbols: Figures indicate ages in Ma (age references in text); Nam — Namurian to Westphalian sediments; Ste — Stephanian sediments; PF — Penninic Front; BF — Briançonnais Front; ESZ — Entrelor Shear Zone; VSZ — Viu-Locana Shear Zone; IL — Insubric Line; 1 — Permian mantle and lower crust; 2 — Permian intrusive; 3 — Permian deposits, including volcanic products.

mate the youngest age of the magmatic component, only the thin needles have been analysed, which belong to the more differentiated types. Four fractions of euhedral needles were analysed by IDTIMS (Fig. 5). They define a discordia with an upper intercept at 281 ± 25 Ma (MSWD = 0.64) and a lower intercept at 68 ± 380 Ma. As for the other samples dated by TIMS, the $^{207}Pb/^{206}Pb$ weighted average age of **277 ± 4 Ma** was adopted. This age is believed to represent a volcanic event, slightly predating the main granite intrusion. This suggests that an unknown part of the Gran Paradiso pre-granite metasediments may derive from magmatic sources of almost the same age as the crosscutting granites.

4. Discussion and conclusions

4.1. Permian age of Gran Paradiso rocks

By combining two complementary approaches – ion probe and isotopic dilution – this study yields interpretable results from complexly zoned zircons. Selecting for IDTIMS analyses only very thin and translucent zircon needles, where bubbles and channels are often observed, has proven to be a successful way to avoid inheritance (Bussy and Cadoppi, 1996). A shortcoming is the relatively low precision because the very small size of the grains precludes abrasion, which is usually efficient in improving concordance. Recent improvements of the conventional approach help in coping with this problem (Paquette and Pin, 2001).

Excluding the younger age of 264 Ma (sample ZH 00 06), interpreted as a minimum age from data of poor quality, two slightly different age groups were determined. Samples ZH 00 05 and ZH 00 13 yield ca. 277 Ma ages, whilst samples ZH 00 14, ZH 00 15 and ZH 98 14 are in the 271–273 Ma age range. There is no obvious explanation for such an age difference, even when compared with the previous 269 ± 6 Ma age determined for the Ecot orthogneiss (Bertrand et al., 2000b).

While the analytical uncertainties vary, all of the age data presented overlap within their error margins (Fig. 6), establishing an middle Permian age for the GP orthogneisses. The two associated metavolcanic rocks are Permian, too. Apart from inherited zircon cores, this study found no pre-Permian material in the massif. The only field evidence for a pre-Permian tectonic and metamorphic evolution are the folded foliations found within enclaves of the less deformed granites (Bertrand, 1968; Callegari et al., 1969; Ballèvre, 1988). Such structures may be related either to pre-Alpine tectonic activity or to syn-emplacement deformation. Though pre-Alpine sillimanite + garnet assemblages have been proven in many places to result from contact metamorphism, they have also been considered remnants of the Variscan orogeny (Callegari et al., 1969; Le Bayon and Ballèvre, 2004). Hereafter, we provisionally hypothesize that the GP orthogneiss protoliths are entirely Permian in age. The age of the host rocks remains questionable, but at least some of them are also Permian. Obviously further geological mapping (Le Bayon, 2005) and further dating are needed, e.g. of the Erfaulet metagranite (cf. 2.3), the Pinerolo formation (2.2), and the Money complex (2.1).

4.2. Permian rocks in the Alps and in western Europe

We mentioned above (2.2) the numerous Permian ages found in the other Piemonte gneiss domes. By contrast, Permian magmatism and especially plutonism are not so frequent in Variscan Europe. Recent reviews of Permian formations in northern and western Europe indicate that 275 Ma was a time of major change (Broutin et al., 1994). Permian deposits are restricted to small, disconnected basins with mostly non-marine deposits. Permian volcanic rocks are widespread in Corsica and are also linked to Permian plutons (Paquette et al., 2003). In the Southern Alps, two „tectono-magmatic and sedimentary" cycles have been proposed (Cortesogno et al., 1998). The older one, during Late Carboniferous to Early Permian times, produced volcanics of calc-alkaline affinity, which might have been controlled by the late-orogenic collapse of the Variscan orogen. Corresponding sediments are mainly of continental origin in the western part, whereas they are mainly marine further East. The younger cycle formations – fluvial red clastic deposits – unconformably overly the early Permian sediments and volcanics, again with a marine tendency toward the East. Magmatic rocks attributed to the younger cycle are alkaline to transitional and may correspond to the early stage of the Tethys extension. From Ivrea to the Carnic Alps, Permian volcanism is dated from 286 to 262 Ma. Such ages overlap with some of the Sesia-Dent Blanche protolith ages (in the 280-290 Ma age range).

In the Helvetic domain, poorly dated Permian formations are probably subject to facies diachronism within several Carboniferous–Permian basins (Aprahamian and Gibergy, 1966). The more differentiated Permian succession in the Western Alps, about 2 km thick, is located in the Briançonnais domain near Briançon (Fabre and Feys, 1966). It comprises light-coloured silicoclastic deposits, rich in limestone lenses and andesite tuffs, unconformably capped by red conglomerates with intercalated rhyolite lavas. Available ages suggest that deposition of the Briançonnais Permian formations took place almost entirely after 275 Ma (Bussy et al., 1996b and personal comm.). Obviously, the Permian magmatism of the Piemonte domes also belongs to the second cycle presented above and is thus linked to the onset of Tethys extension rather than to the Variscan orogeny itself.

In trying to compare the pre-Alpine basement units within the Alpine paleogeographic domains, a Permian reconstitution is proposed in Fig. 7. Paleozoic protoliths being a major part of present-day outcrops, the Paleozoic age pattern appears to be of Alpine paleogeographic interest. Five „blocks" are provisionally proposed, separated on the disputable basis of Alpine paleogeographic and/or tectonic domains (main references quoted above). In the Helvetic domain, 330–340 Ma old Mg-granitoids (with some older orthogneisses) and ca. 305 Ma Fe-granites (Mont Blanc) dominate; Stephanian and Permian sediments are restricted to subordinate basins. GSB shows many ca. 500 Ma old orthogneisses together with thick Namurian to Permian deposits associated with Permian volcanism (and a few granites). In the Internal Penninic domain, Permian volcanics and orthogneisses dominate with a few, poorly dated Carboniferous sediments and some granites (e.g. Brossasco). The Austro-Alpine domain (and Margna-Sesia fragment according to Schmid et al., 2004) is sketched in Fig. 7 as a large mass of 520–

450 Ma old basement with Variscan (not quoted) to Permian granitoids and gabbros, and with possible Permian metavolcanics (gneiss minuti). Concerning the Apulian plate, the Permian high-grade metamorphism of the Ivrea zone corresponds to a lower crustal fragment, and in the Serie dei Laghi a Lower Paleozoic upper crust is capped by felsic volcanism of Permian age. The present-day section (Fig. 7b) shows the location of these „blocks" in a classical section inspired from Schmid and Kissling (2000) and outlines the very small proportion of Mesozoic material included in the Alpine belt.

To conclude, a key point for comparing the origin of the various ICM with pre-Alpine basement from Europe or Apulia is obviously the age range of their orthogneiss protoliths. The Piemonte gneiss domes have classically been attributed to a subducted European margin (Battiston et al., 1985; Benciolini et al., 1984; Ballèvre, 1988; Avigad et al., 1993; Dal Piaz, 1999; Froitzheim, 2001; Ballèvre and Le Bayon, 2004) or to the internal part of a Briançonnais terrane (Schmid and Kissling, 2000; Schmid et al., 2004). An implied assumption is that the Briançonnais terrane is of European origin, which is not unanimously accepted. Admitting the allochthonous character of Briançonnais (GSB) and Piemonte basements with respect to Europe (Stampfli et al., 1998), the extensive Permian magmatism documented may suggest an Apulian signature. It is thus tempting to correlate the ICM (Gran Paradiso, Monte Rosa and Dora Maira) with the Apulian rather than the European plate. The Briançonnais domain is characterised by thick clastic and volcanic formations, of Carboniferous to Permian age. There is thus a strong possibility that the Piemonte gneiss domes, given their impressive Permian magmatism, may represent either the eastern edge of the Briançonnais micro-continent, or a separate terrane initially located in-between Briançonnais and Apulia. In the first option, the occurrence of formations, which may be compared with the Briançonnais Upper Carboniferous at the deepest level of the domes (Money, Pinerolo), is easily explained.

Acknowledgements

The authors are very grateful for a BQR grant from Université de Savoie and for the analytical help of two laboratories: LGCA, UMR-CNRS 5025 Grenoble and Chambéry and „Magmas et Volcans", UMR-CNRS 6524 Clermont-Ferrand. R. Armstrong and the PRISE staff (ANU, Canberra) are gratefully thanked for their help with SHRIMP dating. JMB thanks Bruno Lombardo for helping to compare observations between both sides of the Italy-France boundary and Gabriel Bertrand for companionship during the sampling in the Tellessio area. F. Brouwer and F. Bussy are acknowledged for their valuable critique and comments that helped to improve the submitted manuscript. The ENTE Parco Nazionale Gran Paradiso (Dr. Michele Ottino) is thanked for allowing field work and rock sampling in the Orco valley.

References

Aprahamian, J. and Gibergy, P. (1966): Présence de débris d'ignimbrites dans les grès permiens des Rouchoux (bordure sud-ouest du Pelvoux, Isère). *C .R. Acad. Sci.*, **262**, 1505–1508.

Avigad, D., Chopin, C., Goffé, B. and Michard, A. (1993): Tectonic model for the evolution of the western Alps. *Geology*, **21**, 659–662.

Ballèvre, M. (1988): Collision continentale et chemins P-T: l'unité pennique du Grand Paradis (Alpes occidentales). *Mém. Doc. Centre Armoricain d'Étude Structurale des Socles, Rennes*, **19**, 340 pp.

Battiston, P., Benciolini, L., Dal Piaz, G.V., De Vecchi, G., Marchi, G., Martin, S., Polino, R. and Tartarotti, P. (1984): Geologia di una traversa dal Gran Paradiso alla zona Sesia-Lanzo in alta Val Soana, Piemonte. *Mem. Soc. Geol. It.*, **29**, 209–232.

Bearth, P. (1952): Geologie und Petrographie der Monte Rosa. *Beitr. geol. Karte Schweiz*, Neue Folge **96**, 94 pp.

Benciolini, L., Martin, S. and Tartarotti, P. (1984): Il metamorfismo eclogitico nel basamento del Gran Paradiso ed in unità piemontesi della valle di Campiglia. *Mem. Soc. Geol. It.*, **29**, 127–151.

Bertrand, J.-M. (1968): Étude structurale du versant occidental du Massif du Grand Paradis (Alpes Graies). *Géologie Alpine*, **44**, 55–87.

Bertrand, J.-M. and Leterrier, J. (1997): Granitoïdes d'âge Paléozoïque inférieur dans le socle de Vanoise méridionale: géochronologie U-Pb du métagranite de l'Arpont (Alpes de Savoie, France). *C.R. Acad. Sci.*, **325**, 839–844.

Bertrand, J.-M., Guillot, F., Leterrier, J., Perruchot, M.-P., Aillères, L. and Macaudière, J. (1998): Granitoïdes de la zone houillère briançonnaise en Savoie et en Val d'Aoste (Alpes occidentales): géologie et géochronologie U-Pb sur zircon. *Geodinamica Acta*, **11**, 33–49.

Bertrand, J.-M., Guillot, F. and Leterrier, J. (2000a): Early Paleozoic U-Pb age of zircons from metagranophyres of the Grand-Saint-Bernard Nappe (zona interna, Aosta Valley, Italy) [English abridged version]. *C.R. Acad. Sci.*, **330**, 473–478.

Bertrand, J.-M., Pidgeon, R.T., Leterrier, J., Guillot, F., Gasquet, D. and Gattiglio, M. (2000b): SHRIMP and IDTIMS U-Pb zircon ages of the pre-Alpine basement in the Internal Western Alps (Savoy and Piemont). *Schweiz. Mineral. Petrogr. Mitt.*, **80**, 225–248.

Black, L.P., Kamo, S.L., Allen, C.M., Aleinikoff, J.N., Davis, D.W., Korsch, R.J. and Foudoulis, C. (2003): TEMORA 1: a new zircon standard for Phanerozoic U-Pb geochronology. *Chem. Geol.*, **200**, 155–170.

Borghi, A., Compagnoni, R. and Sandrone, R. (1994): Evoluzione termo-tettonica alpina del settore settentrionale del massiccio del Gran Paradiso (Alpi Occidentali). *Atti Tic. Sci. Terra, Pavia Spec.* ser., **1**, 137–152.

Broutin, J., Cabanis, B., Châteauneuf, J.-J. and Deroin, J.-P. (1994): Évolution biostratigraphique, magmatique et tectonique du domaine paléotéthysien occidental (SW de l'Europe): implications paléogéographiques au Permien inférieur. *Bull. Soc. géol. Fr.*, **165**, 163–179.

Brouwer, F.M., Vissers, R.L.M. and Lamb, W.M. (2002): Structure and metamorphism of the Gran Paradiso massif, western Alps, Italy. *Contrib. Mineral. Petrol.*, **143**, 450–470.

Buchs, A., Chessex, R., Krummenacher, D. and Vuagnat, M. (1962): Ages „plomb total" déterminés par fluorescence X sur les zircons de quelques roches des Alpes. *Schweiz. Mineral. Petrogr. Mitt.*, **42**, 295–305.

Bussy, F. and Cadoppi, P. (1996): U-Pb zircon dating of granitoids from the Dora-Maira massif (western Italian Alps). *Schweiz. Mineral. Petrogr. Mitt.*, **76**, 217–233.

Bussy, F., Derron, M.-H., Jacquod, J., Sartori, M. and Thélin, P. (1996a): The 500 Ma-old Thyon metagranite: a new A-type granite occurrence in the western Penninic Alps (Wallis, Switzerland). *Eur. J. Min.*, **8**, 565–575.

Bussy, F., Sartori, M. and Thélin, P. (1996): U-Pb zircon dating in the middle Penninic basement of the Western Alps (Valais, Switzerland). *Schweiz. Mineral. Petrogr. Mitt.*, **76**, 81–84.

Bussy, F., Venturini, G., Hunziker, J. and Martinotti, G. (1998): U-Pb ages of magmatic rocks of the western Austroalpine Dent-Blanche-Sesia Unit. *Schweiz. Mineral. Petrogr. Mitt.*, **78**, 163–168.

Callegari, E., Compagnoni, R. and Dal Piaz, G.V. (1969): Relitti di strutture intrusive erciniche e scisti a sillimanite nel Massicio del Gran Paradiso. *Boll. Soc. Geol. It.*, **88**, 59–69.

Chessex, R., Delaloye, M., Krummenacher, D. and Vuagnat, M. (1964): Nouvelles déterminations d'âges „plomb total" sur des zircons alpins, 2ème série. *Schweiz. Mineral. Petrogr. Mitt.*, **44**, 43–60.

Chopin, C. (1979): De la Vanoise au massif du Grand Paradis. Une approche pétrographique et radiochronologique de la signification géodynamique du métamorphisme de haute pression. Unpubl. mem., Thèse 3ème cycle Univ. Paris 6, 188 pp.

Compagnoni, R. and Prato, R. (1969): Paramorfosi di cianite su sillimanite in scisti pregranitici del massicio del Gran Paradiso. *Boll. Soc. Geol. It.*, **88**, 537-549.

Compagnoni, R. and Lombardo, B. (1974): The alpine age of the Gran Paradiso eclogites. *Rend. Soc. It. Min. Petrol.*, **30**, 223–237.

Compagnoni, R., Elter, G. and Lombardo, B. (1974): Eterogeneità stratigraphica del complesso degli „Gneiss Minuti" nel massicio cristallino del Gran Paradiso. *Mem. Soc. Geol. It.* **13**, suppl. 1, 227–239.

Compston, W., Williams, I.S., Kirschvink, J.L., Zhang, Z. and Ma, G. (1992): Zircon U-Pb ages for the Early Cambrian timescale. *J. Geol. Soc. London*, **149**, 171–184.

Cortesogno, L., Cassinis, G., Dallagiovanna, G., Gaggero, L., Oggiano, G., Ronchi, A., Seno, S. and Vanossi, M. (1998): The Variscan post-collisional volcanism in Late Carboniferous-Permian sequences of Ligurian Alps, Southern Alps and Sardinia (Italy): a synthesis. *Lithos*, **45**, 305–328.

Cumming, G.L. and Richards, J.R. (1975): Ore lead isotopic ratios in a continuously changing Earth. *Earth Planet. Sci. Lett.*, **28**, 155–171.

Dal Piaz, G.V. (1999): The Austroalpine-Piedmont nappe stack and the puzzle of Alpine Tethys. *Mem. Sci. Geol. Padova*, **51**, 155–176.

Dal Piaz, G.V. and Lombardo, B. (1986): Early Alpine eclogite metamorphism in the Penninic Monte Rosa-Gran Paradiso basement nappes of the northwestern Alps. *Geol. Soc. Am. Mem.*, **164**, 249–265.

Davis, D.W., Williams, I.S. and Krogh, T.E. (2003): Historical development of zircon geochronology. *Reviews in Mineralogy and Geochemistry*, **53**, 145–181.

Delle Piane, L., Perello, P., Compagnoni, R., Baietto, A., Momo, P. and Rolfo, F. (2002): Metamorphic and structural evolution of the Gran Paradiso massif in the Orco valley, western Italian Alps. *81a Riunione estiva della Soc. Geol. Ital., Torino*, 131–132.

D'Amico, C. and Rotura, A. (1982): Occurrence of late-Hercynian peraluminous granites in the Southern Alps. *Rend. Soc. It. Min. Petrol.*, **38**, 27–33.

Elter, G. (1972): Contribution à la connaissance du briançonnais interne et de la bordure piémontaise dans les Alpes Graies nord-orientales et considérations sur les rapports entre les zones du briançonnais et des Schistes lustrés. *Mem. Ist. Geol. Min. Univ. Padova*, **28**, 1–20.

Engi, M., Scherrer, N.C. and Burri, T. (2001): Metamorphic evolution of pelitic rocks of the Monte Rosa nappe: Constraints from petrology and single grain monazite age data. *Schweiz. Mineral. Petrogr. Mitt.*, **81**, 305–328.

Fabre, J. and Feys, R. (1966): Les séries bariolées du massif de Rochachille. Leurs rapports avec le Verrucano de Briançon et les „Permiens" de Maurienne et de Tarentaise. *Atti del Symposium sul Verrucano, Pisa, settembre 1965*, 143–169.

Froitzheim, N. (2001): Origin of the Monte Rosa nappe in the Pennine Alps – A new working hypothesis. *Geol. Soc. Am. Bull.*, **113**, 604–614.

Gebauer, D., Schertl, H.-P., Brix, M. and Schreyer, W. (1997): 35 Ma old ultrahigh-pressure metamorphism and evidence for very rapid exhumation in the Dora Maira Massif, Western Alps. *Lithos*, **41-3**, 5–24.

Giorgis, D., Thélin, P., Stampfli, G. and Bussy, F. (1999): The Mont-Mort metapelites: Variscan metamorphism and geodynamic context (Briançonnais basement, Western Alps, Switzerland). *Schweiz. Mineral. Petrogr. Mitt.*, **79**, 381–378.

Guillot, F., Ploquin, A., Raoult, J.F. and Peruccio-Parison, M.D. (1986): Les séries antépermiennes de Vanoise septentrionale (zone briançonnaise, Alpes de Savoie): lithologie et géochimie dans le massif de Bellecôte; arguments pour un âge antéhouiller. *C.R. Acad. Sci.*, **303**, 1141–1146.

Guillot, F., Liégeois, J.-P. and Fabre, J. (1991): Late Cambrian Mt Pourri granophyres, first dating by U-Pb on zircon of a basement in the internal French Alps (Penninic Alps, Briançonnaise Zone, Vanoise). *C.R. Acad. Sci.*, **313**, 239–244.

Guillot, F., Schaltegger, U., Bertrand, J.M., Deloule, E. and Baudin, T. (2002): Zircon U-Pb geochronology of Ordovician magmatism in the polycyclic Ruitor Massif (Internal W-Alps). *Int. J. Earth Sci.*, **91**, 964–978.

Jaffey, A.H., Flynn, K.F., Glendenin, L.E., Bentley, W.C. and Essling, A.M. (1971): Precision measurement of half-lives and specific activities of 235U and 238U. *Physics Review Section C, Nuclear physics*, **4**, 1889–1906.

Köppel, V. and Grünenfelder, M. (1975): Concordant U-Pb ages of monazite and xenotime from the Central Alps and the timing of high temperature metamorphism, a preliminary report. *Schweiz. Mineral. Petrogr. Mitt.*, **55**, 129–132.

Le Bayon, B. (2005): Evolution structurale et métamorphique d'une croûte continentale subductée (Grand Paradis, Alpes occidentales). Unpubl. Mem., Thèse Doct. Univ. Rennes 1, no. 3315, 379 pp.

Le Bayon, B. and Ballèvre, M. (2004): Field and petrological evidence for a Late Paleozoic (Upper Carboniferous-Permian) age for the Erfaulet orthogneiss (Gran Paradiso, Western Alps). *C. R. Geoscience*, **336**, 1079–1089.

Liati, A., Gebauer, D., Froitzheim, N. and Fanning, C.M. (2001): U-Pb SHRIMP geochronology of an amphibolitized eclogite and an orthogneiss from the Furgg zone (Western Alps) and implications for its geodynamic evolution. *Schweiz. Mineral. Petrogr. Mitt.*, **81**, 379–393.

Ludwig, K.R. (2000): SQUID 1.0, A user's manual. *Berkeley Geochronological Center Special Publication*, **vol. 2**, Berkeley CA, 17 pp.

Marquer, D., Challandes, N. and Schaltegger, U. (1998): Early Permian magmatism in Briançonnais terranes: Truzzo granite and Roffna rhyolite (eastern Pennine nappes, Swiss and Italian Alps). *Schweiz. Mineral. Petrogr. Mitt.*, **78**, 397–414.

Michard, A. and Goffé, B. (2005): Recent advances in Alpine studies: tracking the Caledonian-Variscan belt in the internal western Alps. *C.R. Geoscience,* **337**, 715–718.

Monjoie, P., Bussy, F., Schaltegger, U., Lapierre, H. and Pfeifer, H.R. (2002): L'intrusion gabbroïque permienne du Mont Collon (284 Ma): un témoin du magmatisme d'extension postorogénique varisque (nappe de la Dent Blanche, Alpes suisses. *19ème Réunion Sci. Terre, Nantes. Soc. géol. Fr. eds (abstract)*, p. 181.

Pangaud, C., Lameyre, J. and Michel, R. (1957): Age absolu des migmatites du Grand Paradis (Alpes franco-italiennes). *C.R. Acad. Sci.*, **245**, 331–333.

Paquette, J.-L., Chopin, C. and Peucat, J.-J. (1989): U-P zircon, Rb-Sr and Sm-Nd geochronology of high- to very-high-pressure meta-acidic rocks from the western Alps. *Contrib. Mineral. Petrol.*, **101**, 280–289.

Paquette, J.L., Montel, J.M. and Chopin, C. (1999): U-Th-Pb dating of the Brossasco ultrahigh-pressure metagranite, Dora-Maira massif, western Alps. *Eur. J. Mineral.*, **11**, 69–77.

Paquette, J.-L. and Pin, C. (2001): A new miniaturized extraction chromatography method for precise U-Pb zircon geochronology. *Chem. Geol.*, **176**, 311–319.

Paquette, J.-L., Ménot, R.-P., Pin, C. and Orsini, J.-B. (2003): Episodic and short-lived granitic pulses in a post-collisional setting: evidence from precise U-Pb zircon dating through a crustal cross-section in Corsica. *Chem. Geol.*, **198**, 1–20.

Pin, C. (1990): Evolution of the lower crust in the Ivrea Zone: a model based on isotopic and geochemical data. In: D. Vielzeuf and P. Vidal (eds); Granulites and Crustal Evolution, Kluwer Academic Publishers, 87-110.

Pupin, J.-P. (1980): Zircon and granite petrology. *Contrib. Mineral. Petrol.*, **73**, 207–220.

Ring, U., Collins, A.S. and Kassem, O.K (2005): U–Pb SHRIMP data on the crystalliyation age of the Gran Paradiso augengneiss, Italian Western Alps: further evidence for Permian magmatic activity in the Alps during break-up of Pangea. *Eclogae geol. Helv.* **98**, 363–370.

Rubatto, D. (1998): Dating of pre-Alpine magmatism, Jurassic ophiolites and Alpine subductions in the Western Alps. Unpublished PHd thesis, ETH Zurich.

Schmid, S.M., Fügenschuh, B., Kissling, E. and Schuster, R. (2004): Tectonic map and overall architecture of the Alpine orogen. *Eclogae geol. Helv.*, **97**, 93–117.

Schmid, S.M. and Kissling, E. (2000): The arc of the western Alps in the light of geophysical data on deep crustal structure. *Tectonics*, **19**, 62–85.

Schuster, R., Koller, F., Hoeck, V., Hoinkes, G. and Bousquet, R. (2004): Explanatory notes to the map: metamorphic structure of the Alps, metamorphic evolution of the Eastern Alps. *Mitt. Österr. Miner. Ges.*, **149**, 175–199.

Stacey, J.S. and Kramers, J.D. (1975): Approximation of terrestrial lead isotope evolution by a two-stage model. *Earth Planet. Sci. Lett.*, **26**, 207–221.

Stampfli, G.M., Mosar, J., Marquer, D., Marchant, R., Baudin, T. and Borel, G. (1998): Subduction and obduction processes in the Swiss Alps. *Tectonophysics*, **296**, 159–204.

Steiger, R.H. and Jäger, E. (1977): Subcommission on geochronology: convention on the use of decay constants in geo- and cosmochronology. *Earth Planet. Sci. Lett.*, **36**, 359–362.

Vavra, G. and Schaltegger, U. (1999): Post-granulite facies monazite growth and rejuvenation during Permian to Lower Jurassic thermal and fluid events in the Ivrea Zone (Southern Alps). *Contrib. Mineral. Petrol.*, 134, 405–414.

Vearncombe, J.R. (1983): High pressure-low temperature metamorphism in the Gran Paradiso basement, Western Alps. *J. Metamorphic Geol.*, **1**, 103–115.

Vialon, P. (1966): Etude géologique du massif cristallin Dora Maira, Alpes cottiennes, Italie. Unpubl. thesis, Grenoble, 293 pp.

Williams, I.S and Claesson, S. (1987): Isotopic evidence for the Precambrian provenance and Caledonian metamorphism of high-grade paragneisses from the Seve Nappes, Scandinavian Caledonides. II: Ion microprobe U-Th-Pb. *Contrib. Mineral. Petrol.*, **97**, 205–217.

Received 18 November 2004
Accepted in revised form 29 June 2005
Editorial handling: M. Engi